Top-pinned soft magnetic underlayer with nano- or oriented-crystalline structure fabricated by electroless plating

著者	齊藤 伸
journal or publication title	Journal of applied physics
volume	102
number	3
page range	033906-1-033906-4
year	2007
URL	http://hdl.handle.net/10097/35009

doi: 10.1063/1.2764205

Top-pinned soft magnetic underlayer with nano- or oriented-crystalline structure fabricated by electroless plating

Atsushi Hashimoto and Shin Saito[a)]
Department of Electronic Engineering, Tohoku University, 6-6-05, Aoba, Aramaki, Aoba-ku, Sendai 980-8579, Japan

Migaku Takahashi
New Industry Creation Hatchery Center, Tohoku University, 6-6-10, Aoba, Aramaki, Aoba-ku, Sendai 980-8579, Japan

Nobuaki Mukai
Toyo Kohan Co., Ltd., Technical Research Laboratory, 1302-2, Oaza Higashitoyoi, Kudamatsu 744-8661, Japan

(Received 27 March 2007; accepted 19 June 2007; published online 3 August 2007)

To suppress both spike noise and wide adjacent track erasure for perpendicular recording media, we have proposed a soft magnetic underlayer (SUL) with the top-type pinning structure, which consists of a soft magnetic layer fabricated by plating and an antiferromagnetic layer deposited by sputtering, on an Al/NiP substrate (top-pinned plated SUL). To realize this concept, plated NiFe layers with random nano-crystalline structure and with (111) sheet texture were achieved using suitable reducers in electroless plating. Magnetic domain structures inside the whole disk for the top-pinned plated SUL prepared under various field-cool conditions reveal that the thermal stability of a single-domain state can be maintained over 130 °C even for a small antiferromagnetic layer thickness of 5 nm.
 [DOI: 10.1063/1.2764205]

I. INTRODUCTION

To achieve a high head field in a perpendicular recording system, a soft magnetic underlayer (SUL) with large thickness (product of saturation magnetic flux density of SUL and thickness, $B_s^{\mathrm{SUL}} \times d_{\mathrm{SUL}}$ larger than 100 T nm) is favorable from the viewpoint of the magnetic flux circuit in writing. The fabrication of a thick SUL was accompanied by serious problems such as the generation of spike noise and wide adjacent track erasure (WATE).[1] For suppressing spike noise, single-domain formation in the whole disk-shape SUL at a zero-field condition is effective by preventing Bloch walls in the SUL.[2] WATE occurs due to concentration of magnetic flux on the edge of the return yoke in writing. Thus, WATE can be suppressed by wide distribution of the magnetic flux around the return yoke, which can be achieved by reducing the susceptibility of the SUL in the film-normal direction ($\chi_\perp$).[3] As a possible solution for eliminating these problems, we have previously proposed SUL with the so-called top-pinned type structure, the concept for which is as follows: 1) The main soft magnetic layer is fabricated by an electroless plating method,[4–6] and 2) An antiferromagnetic (AFM) layer is sputtered on plated soft magnetic film so as to form single domain in the whole disk-shape SUL at zero field (see Fig. 1).[4] In case of the top-pinned type SUL with a single-domain structure, $\chi_\perp$ around the SUL surface can be lowered since strong unidirectional anisotropy is induced near the SUL/AFM interface.[7]

In this paper, we investigate a plated soft magnetic film with nano-crystalline or oriented-crystalline structure, and report thermal stability for a single-domain SUL utilizing the plated soft magnetic film.

II. EXPERIMENTAL PROCEDURE

NiFe was selected as the main SUL material and was electroless-plated on a 2.5-inch diameter Al/NiP disk substrate. For the plating, NaH_2PO_2 and dimethylamine-borane (DMAB) were suitably used as reducers. Details of the plating conditions are summarized in Table I. The plated NiFe films of $1-2$ μm thickness were polished, and then the designed thicknesses of several 10 to 300 nm were obtained with the surface roughness (R_a) less than 0.3 nm. Prior to sputtering, the surface of the plated film was etched using Ar plasma to remove absorbed impure gas on the surface. After etching, $Co_{70}Fe_{30}$(8 nm) or NiFe(3 nm)/$Co_{70}Fe_{30}$(8 nm) and an AFM layer were deposited using dc-magnetron sputtering. $Mn_{83}Ir_{17}$ with fcc structure was used as the AFM material. To induce unidirectional magnetic anisotropy by mini-

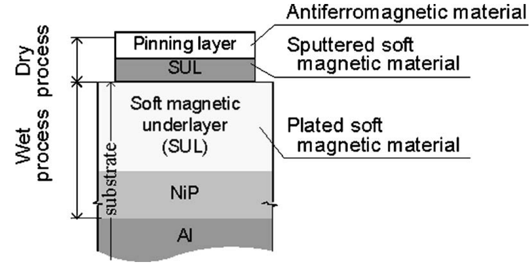

FIG. 1. Schematic view of the stacking structure and corresponding fabrication method for proposed top-pinned-type SUL using plated soft magnetic layer.

[a)]Electronic address: ssaito@ecei.tohoku.ac.jp

TABLE I. Electroless-plating conditions for normal, nano-crystalline, and oriented-crystalline NiFe layer.

	Normal NiFe	Nano-crystalline NiFe	Oriented-crystalline NiFe
$NiSO_4$ (g/L)	13	2.6	13
$FeSO_4$ (g/L)	28	5.7	28
Reducer (g/L)	NaH_2PO_4:5.5	DMAB: 1.0	NaH_2PO_4:5.5
Complex agent	Adequate	Adequate	Adequate
pH	9.6	9.5	9.6
Bath temperature (°C)	80	70	80
Deposition rate (μm/h)	4.0	1.5	4.0
Plated seed layer	-	Ni	Co

mizing distribution of AFM spin directions, AFM layer was aligned high symmetrical plane of (111) sheet texture.[8] After sputtering, a cooling treatment under a static magnetic field from 200 °C was carried out. In this treatment, the applied magnetic field was 600–800 Oe toward the disk radial direction. Detailed process is explained in Sec. III C in this paper. The structures were examined by cross-sectional transmission electron microscope (TEM). The hysteresis loops were measured using magneto-optical Kerr equipment (MOKE) with the applied field parallel to the disk radial direction. Note that the MOKE hysteresis loops reflect the magnetization up to a depth of about 20 nm from the film surface due to the penetration depth of the probe light (wavelength: 633 nm). The domain structure of the whole disk was observed by scanning optical polarization.

III. RESULTS AND DISCUSSION

A. Growth mode of the plated NiFe layer on a NiP layer

First, the growth mode of the plated NiFe layer on an amorphous NiP layer was investigated. Figure 2 shows a bright field TEM image of a plated NiFe layer on an Al/NiP disk utilizing NaH_2PO_2 as a reducer. A 10-nm-thick NiFe layer was sputtered on top of the plated NiFe layer. At the bottom of the plated NiFe layer, lattice stripes and grain boundaries were not clearly observed. Hereafter, this layer

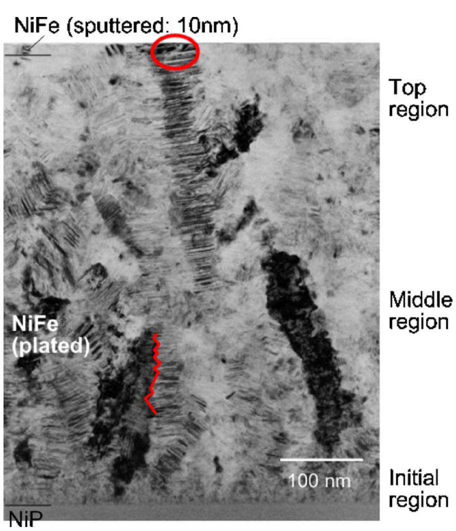

FIG. 2. (Color online) Bright field TEM image for Al/NiP/plated NiFe/sputtered NiFe sample.

will be called the initial growth layer. For the middle part of the plated NiFe layer, the lattice stripes of each NiFe grain continue in random directions, and the shapes of the grain boundaries were not straight but zigzagged back and forth. At the top of the plated NiFe grains, lattice stripes were aligned parallel to the film surface. According to electron diffraction patterns, lattice stripes in the bright field image originated from the diffraction of the (111) planes of the NiFe grains. Therefore, the growth mechanism of the plated NiFe grains on an amorphous NiP layer was clarified as follows. 1) In the initial growth stage, a Fe^{2+} or Ni^{2+} receives electrons from reducers at the interface between plating solution and the amorphous NiP surface, 2) the initial nuclei are generated with crystal axes randomly oriented three-dimensionally, 3) each grain grows toward the preferred $\langle 111 \rangle$ direction, and growth competition with neighboring grains occur, and 4) finally only grains with $\langle 111 \rangle$ axes parallel to the film normal direction grow continuously. In this study, lattice stripes continue from the plated NiFe grains to the sputtered NiFe grains, as seen in the crystal structure near the interface between the sputtered and plated layers (circle in Fig. 2). This result indicates that the sputtered NiFe grains glow epitaxially on the plated NiFe grains. Therefore, in order to form AFM grains with (111) sheet texture on the plated NiFe film, two methods are considered. The first is nano-crystallization of the plated NiFe. In this case, the sputtered buffer layer is needed to control the crystallographic orientation of an AFM layer. And second is oriented crystallization of the plated NiFe with (111) sheet texture. In this case, a plated seed layer is needed to control crystallographic orientation.

B. Nano-crystalline NiFe layer

In order to reduce the plated grain size below several nanometers, boron addition using a reducer is known to be effective for Co-Ni-Fe alloy.[9] We attempted to add boron to NiFe using DMAB as a reducer. In general, for electroless plating, the oxidization-reduction potential (ORP) of the plating surface must be less than the ORP of plating material. Since reduction power of DMAB is weaker than that for NaH_2PO_2, the ORP of NiFe is lower than that of NiP. Thus, Ni, with an ORP was lower than NiP, was selected as the seed material. Figure 3 shows a bright field TEM image of a plated NiFeB layer. The inset shows an electron diffraction pattern (EDP) from the NiFeB layer obtained using a 120-nm-probe spot. Judging from the bright field image, although

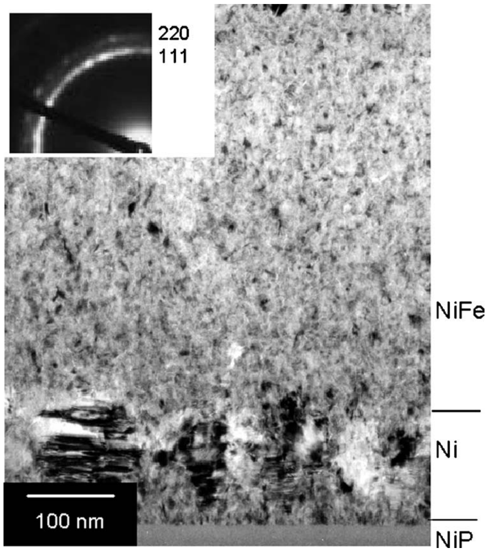

FIG. 3. Bright field TEM image of the plated NiFe layer utilizing the DMAB reducer on a plated Ni seed layer. The inset shows the electron diffraction image of the plated NiFe layer using the 120-nm-probe spot.

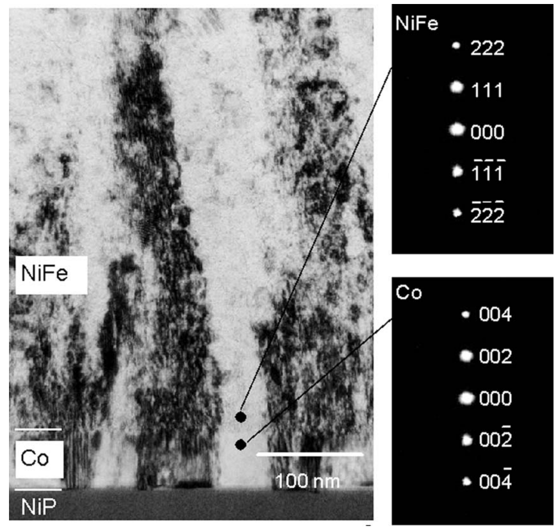

FIG. 4. (Left) Bright field TEM image for the plated NiFe layer utilized NaH_2PO_2 reducer on the plated Co seed layer. (Right) Electron diffraction patterns for (top) NiFe and (bottom) Co layer, respectively, using a 1-nm-probe spot.

the grain diameter in the seed layer was larger than several tens of nm, the average diameter of the NiFe grains was about 5–6 nm. The EDP reveals a ring pattern, which indicates that NiFe grains have three dimensional random orientations. These results indicate that boron addition using DMAB is effective for reducing the plated grain size of NiFe. Magnetic properties, such as H_c and B_s, for this SUL can be designed from 2–5 Oe and from 0.7–1.5 T, respectively, by adjusting plating conditions.

C. Oriented crystalline NiFe layer

In order to form oriented crystalline NiFe, It is essential that crystallographic orientation of the seed layer can be controlled by the plating process. Based on our trials of various materials with a fcc or hcp structure (such as Cu, Ni, Co, Ru, Ir, Au, and Pd) plated on an Al/NiP substrate, only the crystal orientation of Co could be controlled from the initial growth. The electroless-plating conditions for Co are listed in Table II. The crystallographic orientation of the plated Co layer can be controlled by changing the amount of NaH_2PO_4. In the case of 0.05 mol/L NaH_2PO_4, the plated Co orient (10.0) plane parallel to the film surface. On the contrary, in the case of 0.20 mol/L NaH_2PO_4, the plated Co completely takes (00.2)-plane sheet texture. Thus, we choose (00.2)-plane oriented Co as the plating seed material. Figure 4 shows a bright field TEM image of a NiFe layer plated on a Co seed layer. The EDPs obtained from the NiFe and Co layers near the Co/NiFe interface by a 1-nm-probe spot, respectively, are also shown. As seen in the bright field image of the Co seed layer, lattice stripes are clearly observed and are parallel to the film plane. Columnar structures with white or black contrast continue from the Co layer into the NiFe layer, as seen in the interface between Co and NiFe layer. The grain diameter of NiFe was found to be 10–12 nm. The EDPs reveal that the hcp (00.2)-plane of Co and the fcc (111)-plane of NiFe are aligned parallel to the film surface. These results indicate that the initial growth of the NiFe layer changes from three-dimensional randomly orientation to a (111)-plane sheet texture since the NiFe layer grows epitaxially on oriented Co seed layer. According to the lattice image of (111) plane, orientation distribution of [111] direction of plated NiFe layer against the film normal is within ±9°. Note that the texture of sputtered $Co_{70}Fe_{30}$/MnIr bilayers on the plated NiFe layer is oriented to the fcc (111) plane judging from TEM analysis.

TABLE II. Electroless-plating conditions for the Co layer on Al/NiP substrate

$CoSO_4$ (mol/L)	0.05
Sodium citrate (mol/L)	0.20
$(NH_4)_2SO_4$ (mol/L)	0.50
Reducer (mol/L)	NaH_2PO_4: 0.05–0.20
pH	10.0
Bath temperature (°C)	80

D. Thermal stability of the single-domain structure for top-pinned type plated SUL

Finally, T_B of the SUL stacked with the AFM layer was evaluated in order to investigate thermal stability of the single-domain structure. We determined T_B by the change in the domain structure of the disk-shape SUL. Figure 5 shows the heating and cooling treatment sequences with and without a magnetic field. Typical domain structures and hysteresis loops after each treatment for the disk-shape SUL are also shown. In the case of the SUL without the AFM layer, shown in Fig. 5(a), after the field-cool treatment to room temperature $(R.T.)$, the domain structure of the whole SUL was divided symmetrically into two areas which have the easy magnetized axis $(E.A.)$ parallel to the disk radial direction. Hereafter, this domain structure is termed the multi-domain structure. On the other hand, in the case of the SUL with AFM layer, shown in Figs. 5(b) and 5(c), unidirectional anisotropy is induced toward the inner or outer direction of

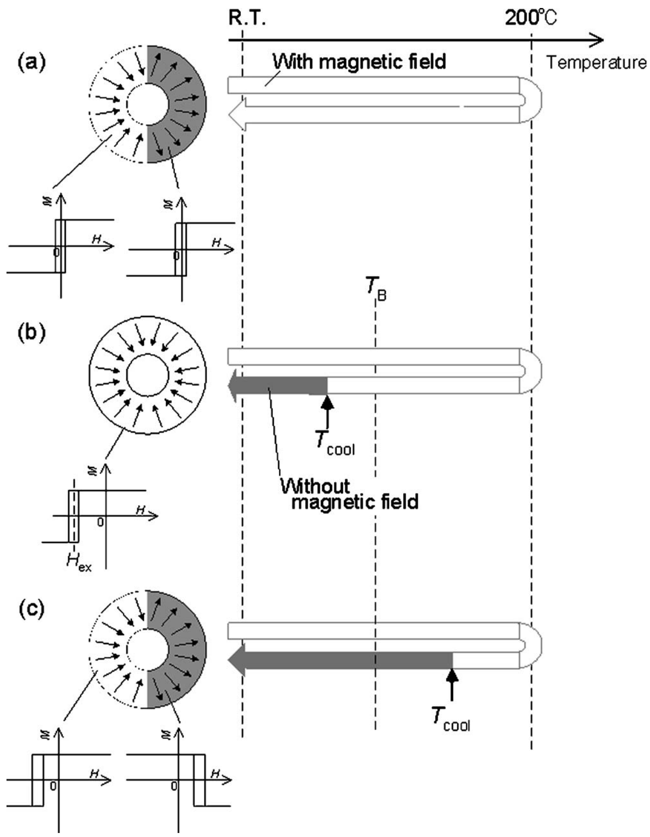

FIG. 5. Heating and cooling treatment sequences with or without magnetic field. (a) disk-shape soft magnetic film. (b), (c) and (d) are for disk-shaped AFM/FM stacked film. Schematic domain structure and hysteresis loops are also shown.

the disk parallel to the SUL moment at T_B. Here, $T_{\rm cool}$ is defined as the temperature at which magnetic field is removed. For $T_{\rm cool} < T_B$ [Fig. 5(b)], SUL moment is saturated toward the outside of the disk radial direction at $T = T_B$. In this case, unidirectional anisotropy is induced toward the outside of the disk radial direction, which results in single-domain formation at the zero-filed state. Exchange bias field (H_{ex}) appeared in the hysteresis loop due to unidirectional anisotropy. In the case of $T_B < T_{\rm cool}$ [Fig. 5(c)], SUL shows a multi-domain structure at $T_{\rm cool}$ since the exchange coupling does not work at the interface between SUL and the AFM layer. When cooled to $R.T.$ without a magnetic field, unidirectional anisotropy was induced along the magnetic moments in each domain, which means that the magnetizations were fixed in two directions; toward the outside and toward the inside along the disk-radial line. As a result, hysteresis loops measured in each domain shift to the opposite side. Therefore, focusing on the domain structure of the disk-shape SUL with an AFM layer, T_B can be evaluated as the boundary temperature of $T_{\rm cool}$ between single and multi domain structure.

Figure 6 shows the $T_{\rm cool}$ dependence of H_{ex} for (a) plated nano-crystalline NiFe/NiFe(3 nm)/$Co_{70}Fe_{30}$(8 nm)/MnIr (5 nm) ($B_s \cdot d_{\rm SUL} = 270$ T nm) and (b) plated oriented-crystalline NiFe/$Co_{70}Fe_{30}$(8 nm)/MnIr(5 nm) ($B_s \cdot d_{\rm SUL}$ $= 380$ T nm) samples. The filled and open symbols represent the single and multi-domain at zero field, respectively. Typical domain structures are also shown in Fig. 6. Note that the brightest part in the domain image along the disk edge is the area without sputter-deposition due to the substrate holder for sputtering. In both (a) and (b), H_{ex} appears and shows a constant value [(a) 43 Oe, and (b) 18 Oe] which is independent of $T_{\rm cool}$. This result reveals that unidirectional anisotropy is induced even for MnIr thickness of 5 nm. T_B is about 130 °C for (a), and 150 °C for (b).

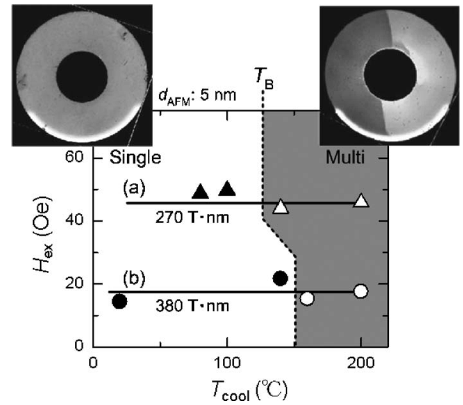

FIG. 6. Change in H_{ex} and domain structure of the whole disk depending on the field-cool temperature for (a) nano- and (b) oriented-crystalline SUL, respectively.

IV. CONCLUSION

To suppress both spike noise and wide adjacent track erasure for perpendicular recording media, we have proposed a soft magnetic underlayer (SUL) with the top-pinned type structure, which consists of a soft magnetic layer fabricated by plating and an antiferromagnetic layer deposited by sputtering, on an Al/NiP substrate (top-pinned plated SUL). To realize this concept, plated NiFe layers with random nanocrystalline structure and with (111) sheet texture were achieved using suitable reducers in electroless plating. Magnetic domain structures inside the whole disk for the top-pinned plated SUL prepared under various field-cool conditions reveal that the thermal stability of a single-domain state can be maintained over 130 °C even for a small antiferromagnetic layer thickness of 5 nm.

[1] S. Li *et al.*, IEEE Trans. Magn. **42**, 3874 (2006).
[2] S. Takahashi, Y. Yamakawa, and K. Ouchi, J. Magn. Soc. Jpn. **23**, 19 (1999).
[3] A. Hashimoto, S. Saito, and M. Takahashi, J. Appl. Phys. **99**, 08Q907 (2006).
[4] S. Saito, A. Hashimoto, M. Takahashi, and N. Mukai, J. Magn. Soc. Jpn. **28**, 289 (2004).
[5] H. Uwazumi, N. Nakajima, M. Masuda, T. Kawata, S. Takenoiri, S. Watanabe, Y. Sakai, and K. Enomoto, IEEE Trans. Magn. **40**, 2392 (2004).
[6] T. Osaka, T. Asahi, T. Yokoshima, and J. Kwaji, J. Magn. Magn. Mater. **287**, 292 (2005).
[7] A. Hashimoto, S. Saito, and M. Takahashi, J. Magn. Magn. Mater. **287**, 287 (2005).
[8] T. Sato, M. Tsunoda, and M. Takahashi, Appl. Phys. Lett. **84**, 5222 (2004).
[9] T. Yokoshima, D. Kaneko, M. Akahori, H. S. Nam, and T. Osaka, J. Electroanal. Chem. **491**, 197 (2000).